MR Neurography and Diffusion Tensor Imaging:

Origins, History & Clinical Impact

by

Aaron Filler, MD, PhD

Institute for Nerve Medicine

2716 Ocean Park Blvd., #3082

Santa Monica, CA 90405

Funding for some portions of this work from the National Institutes of Health and from the Wellcome Trust are noted in the Acknowledgements, and therefore public access depository placement of this article is requested.

Corresponding Author:

Aaron G. Filler, MD, PhD

Medical Director

Institute for Nerve Medicine

2716 Ocean Park Blvd. #3082

Santa Monica, CA 90405

USA

e-mail: afiller@nervemed.com

cell: 1 310 621-1983

office: 1 310 314-6410

fax: 1 310 664-1916

No changes of address are expected

Abstract

MR Neurography and Diffusion Tensor Imaging: Origins, History & Clinical Impact of the first 50,000 cases with an Assessment of Efficacy and Utility in a Prospective 5,000 Patient Study Group

Objective – Methods were invented that made it possible to image peripheral nerves in the body and to image neural tracts in the brain. Over a 15 year period, these techniques – MR Neurography and Diffusion Tensor Imaging – were then deployed in the clinical and research community and applied to about 50,000 patients. Within this group, about 5,000 patients having MR Neurography were carefully tracked on a prospective basis.

Method – In the study group a uniform imaging methodology was applied and all images were reviewed and registered by referral source, clinical indication, efficacy of imaging and quality. Various classes of image findings were identified and subjected to a variety of small targeted prospective outcome studies. Those findings demonstrated to be clinically significant were then tracked in the larger clinical volume data set.

Results – MR Neurography demonstrates mechanical distortion of nerves, hyperintensity consistent with nerve irritation, nerve swelling, discontinuity, relations of nerves to masses, and image features revealing distortion of nerve at entrapment points. These findings are often clinically relevant and warrant full consideration in the diagnostic process. They result in specific pathologic diagnoses that are comparable to electrodiagnostic testing in clinical efficacy.

Conclusions – MR Neurography and DTI neural tract imaging have been validated as indispensable clinical diagnostic methods that provide reliable anatomical pathological information. There is no alternative diagnostic method in many situations. With the elapse of 15 years, tens of thousands of imaging studies, and hundreds of publications, these methods should no longer be considered experimental.

Running Title: Neurography and Diffusion Tensor Imaging

Key words: Brachial Plexus, Brain, DTI, MRI, Nerve, Piriformis, Thoracic Outlet

MR Neurography and Diffusion Tensor Imaging: Origins, History & Clinical Impact of the first 50,000 cases with an Assessment of Efficacy and Utility in a Prospective 5,000 Patient Study Group

Aaron Filler, MD, PhD, FRCS

Neurography Institute, Santa Monica, CA

Introduction

The discovery of a series of MR pulse sequence strategies for tissue specific imaging of nerve and nerve tracts in 1991 and 1992 has opened a new diagnostic world in which a wide variety of pathologies involving nerves and neural tracts can be visualized directly these techniques are grouped under the terms “MR Neurography” (MRN) for peripheral nerve and “Diffusion Tensor Imaging” (DTI) or “Tractography” for the CNS. Many specialists in these two fields are unaware that they have a common origin in a shared set of fundamental imaging strategies and algorithms that grew out of a unitary development project.

The first DTI image using multi-dimensional directional information to show curved neural tracts traversing the brain (Fig. 1) and the first neurography images were submitted in a series of UK patent descriptions by Filler et al between March and July of 1992 and were published by the World Intellectual Property Organization in 1993 . Related images were published in the proceedings of the Society for Magnetic Resonance in Medicine annual meeting in Berlin in August of 1992 .

Prior to these developments in 1992, it had been generally assumed among radiologists that peripheral nerve simply could not be imaged reliably. The potential to use diffusion MRI to tract trace through the brain was also not really anticipated in the clinical community. The strategy of using diffusion based MRI imaging sequences to help produce linear neural images was first discussed by Filler et al in 1991, and emerged as a workable technique through discoveries by Filler, Howe and Richards (in London and Seattle) in late 1991 and by LeBihan and Basser (in Bethesda) in early 1992.

This represented a fundamental rethinking of neurological imaging data that transformed the legacy of cross sectional imaging from CT scanning that had been the conceptual basis of MRI into the realm of tract tracing that had dominated neuroanatomical research in the 1970's and 1980's. Interest in tract tracing for evolutionary studies of uniquely human neuroanatomical structures in the brain related to speech and in the periphery related to the lumbar reorganization in hominoids provided

the original impetus for development of imageable tractographic methods for CNS and nerve.

Previously, the methodology of MRI had been directed at identifying methods to assign contrasting image intensities to various voxels (three dimensional pixels) in an MRI image slice. This was accomplished by a wide array of pulse sequences that manipulated aspects of the T1 and T2 relaxation time of protons. Positional information on the voxels was obtained by using magnetic gradients to assign unique magnetic field strengths to each location in the volume to be imaged, then using Fourier transforms to extract signal strength data from each voxel at various echo times after a simple or complex radiofrequency pulse. Diffusion NMR *per se* was also known for decades – it acted as yet another source of obtaining contrast on the voxels by assessing relaxation rates (signal decays) that related to the degree to which nerve fibers tended to have water diffuse anisotropically (in a primary direction) rather than isotropically (in all directions) . This is the basis for the diffusion weighted imaging (DWI) that has been used to detect strokes for many years .

In MR angiography, we typically produce a series of image slices in which blood vessel voxels are bright and then reconstruct the vessel tree from a stack of slices with vessels shown prominently in each cross section. DTI works very differently. The critical insight was a modification in the fundamental data acquisition process of the MRI

scanning system so that each voxel would yield not only image intensity data, but also directional data showing the tensor (3D complex vector) direction in three dimensional space.

Each voxel could be represented by a small arrow pointed in the direction of the principal nerve orientation in that volume. Instead of producing a cross section with dots, we produce an array of directional arrows along neural tracts and these can be strung together by various standard 3D graphics techniques to produce linear images of nerve tracts. In addition, pulse sequence modifications could be applied that made this data discoverable in peripheral nerve as well. The resulting neurograms then served as a model for discovering additional non-diffusion tractographic methods for peripheral nerve.

By 1993, there were several major publications in these fields . In the subsequent fifteen years, over a hundred academic publications have reported on various aspects of this new imaging modality in peripheral nerve including several large scale formal outcome assessment trials . Nonetheless, most textbooks of radiology or neuroradiology do not devote any pages at all to nerve imaging , as if nerves were not a clinically significant part of the body. Most practicing physicians still do not appreciate that high quality diagnostically efficacious nerve imaging is available.

More than 2,000 studies have been published that explore DTI tractography in the central nervous system although most of this has been in the past three years. The

clinical impact of DTI is still difficult to predict. However, it encodes a great deal of information that is usually discarded in the course of CNS imaging. Because of this it has shown great promise for detecting subtle derangements of brain architecture that are difficult to appreciate with cross sectional imaging.

Formal outcome studies on the use of DTI for evaluation of traumatic brain injury , in predicting outcome after intracerebral hemorrhage , and for surgical guidance to optimize glioma resection have appeared along with numerous preliminary studies for a wide variety of clinical uses in neuroscience such as in the evaluation of dementia in Alzheimer's and in identifying subtle lesions involved in the etiology of epilepsy . Recent diffusion image presentation algorithms have also been used to further advance earlier work on the use of diffusion tensor imaging for peripheral nerve .

In the smaller but more clinical peripheral nerve imaging arena, MR Neurography has proven to be more efficacious than electrodiagnostic studies for identifying nerve compressions that will improve with surgical treatment. This has proven to be true both in diagnoses that are typically evaluated by electrodiagnostics such as carpal tunnel syndrome and also in diagnoses in which electrodiagnostics have proven difficult to rely on such as piriformis syndrome and related sciatic nerve entrapments .

Utility for MR Neurography has now been established in evaluation of entrapment syndromes , nerve injury/evaluation of repair , nerve tumor assessment , as well as in the setting of neuritis and a variety of neuropathies . It has also proven

effective for evaluating nerve disorders affecting the young pediatric patient such as obstetrical brachial plexus palsy.

Over the 15 years since MR Neurography was initially brought into clinical use, about 25,000 peripheral nerve imaging studies have been conducted. DTI can be estimated to have been performed in conjunction with brain MRI scans in tens of thousands of patients mostly in the past two years. This report assesses utilization and diagnostic range for MR Neurography in a prospective group of more than 5,000 patients for whom standardized protocols were applied, research consent obtained, and clinical data collected and organized.

For both T2-Neurography and DTI, the clinical results can be used to help verify hypotheses about the physical basis of the underlying biophysical phenomena that result in the observed image effects in both normal and pathological situations. In addition, by identifying the most effective parameters to optimize, the clinical results can best identify the way forward for future developments.

Methods

All patients had physical examination to identify a specific suspect nerve pathology. Images were ordered through St. George's Hospital Medical School (1992 to 1996) University of Washington Department of Radiology (1993 to 1995), UCLA or OliveView/UCLA Department of Radiology (1996 to 2001) or the Neurography Institute (2000 to 2007). Image protocols included matched T1 (anatomic) and neurographic image pulse sequences in multiple planes including at least one "nerve perpendicular" plane for fascicle assessment. For all MRN studies echo times were greater than 40 milliseconds (usually 70 to 100 ms) in order to assure that no magic angle effects could occur . Referral biases towards these specialty centers due to their widely recognized expertise in this area was an unavoidable aspect of the data.

Results

I. T2-based MR Neurography

Physical Basis

The clinical pathology data in T2 based MR Neurography appears to derive from alterations in endoneurial fluid content in nerve. This fluid appears to be the sole candidate for the class of water to which the applied image parameters should apply. It is a low protein fluid (long T2), confined to the endoneurium of nerve fascicles (Fig 2), that physiologically participates in a bulk proximal to distal flow. Compressions or irritative

processes appear to be capable of increasing the amount of this fluid relative to the other cellular components of the fascicle in a variety of pathological conditions.

Utilization by type of pathology:

The dominant class of pathology for which MRN studies were ordered in this group were in the area of nerve entrapment. Utilization in tumor (Fig 3 and 4), trauma (Fig 5), and neuropathy represented only a very small percentage of the studies. However, this also reflects the relative incidence of these conditions. Nerve entrapment/degenerative problems such as carpal tunnel, piriformis syndrome, thoracic outlet syndrome and radicular spinal syndromes are far more prevalent. When correction for incidence of the major classes of disorders is considered, the utilization pattern appears to be similar for degenerative/pain/entrapment, neoplastic, and traumatic nerve pathology. Our study participants represented about 0.01% of the total incidence for the time period for these types of cases. Utilization for the evaluation of neuropathy is very low.

Utilization by body region/nerve

Use of MR Neurography is heavily concentrated in the evaluation of large proximal nerves that are difficult to assess accurately by routine electrodiagnostic techniques and physical exam. Studies of the lumbosacral plexus, proximal sciatic nerve and other pelvic nerves (ilioinguinal, pudendal, femoral, obturator) constituted about 42% of cases. Brachial plexus imaging accounted for an additional 18% of cases and lumbar spinal nerve studies were 5%. The remaining 35% were studies of knee/peroneal nerve, elbow/ulnar nerve, wrist/median nerve, ankle/tibial nerve, upper neck/occipital nerves, thigh/distal sciatic, calf, foot, upper arm, abdominal wall, face, intercostals, and various individual study types.

Utilization by practitioner category

Most MR neurography studies were ordered by neurosurgeons (43%) and this appeared to represent a combined influence of diagnostics and surgical planning. Surgical planning as a reason for ordering was inferred when the study was ordered by a surgeon and the diagnosis was already established. Neurologists ordered an additional 21% of the studies, while pain specialists (12%), physiatrists (8%), orthopedic surgeons (6%) and

various others ordering the remaining studies. Only a very small number were ordered for pediatric patients and these generally were not ordered by pediatricians.

Diagnostic efficacy and ordering

MR Neurography had a high diagnostic efficacy. More than 96% of studies resulted in either specific findings involving the nerve of interest or in a definitive statement that the nerve or nerves in question were entirely normal in appearance. The remaining 4% of studies were non-diagnostic because of movement, artifact from implants, body habitus or pain limiting appropriate positioning in the scanner, or ordering errors. Ordering errors arose because many practitioners were not experienced in ordering nerve imaging. For example, a neurologist or neurosurgeon (or staff member) seeking to evaluate sciatica due to piriformis syndrome would order a lumbar MRN instead of the necessary pelvic MRN because of the habit of using lumbar MRI for sciatica.

Contrast use

Intravenous gadolinium contrast was used in about 0.4% of cases. Where tumor was part of an initial differential diagnosis but not proven, contrast was not used. Only patients with known tumors received intravenous contrast.

Follow up imaging studies

About 1% of the studies were part of a repetitive set. These were generally patients who had a diagnostic MRN and then were referred for repeat imaging when symptoms recurred after treatment, extended time elapsed between initial imaging and treatment, when recurrent tumor was suspected, or when new symptoms arose in the same body region. Generally, the use of repetitive imaging was lower that what has been reported for lumbar or cervical MRI.

Geographic distribution

The highest utilization of MR Neurography was in Southern California – accounting for about 82% of patients imaged. Usage was lower in other regions with the only other significant concentration being Northern California with the remainder coming from nearly all US States, England, Spain, France, Japan, Mexico and China.

Classes of image findings:

Image findings in MR Neurography studies include the presence of regions of nerve hyperintensity, distortions of normal nerve course, abnormal contours and alterations of nerve caliber (Figs 6 & 7) – any of which can be classed by the degree or severity of the abnormality. These findings seem most reliable for the larger named nerves over 3 mm in diameter although there is no technical limit on the imageable size of a nerve. In trauma, assessments of nerve continuity (Fig 5) and/or location of severed nerve endings are feasible although edema at a site of injury limits the utility of MR Neurography in acute injury settings, but this becomes less of an issue after the elapse of two to four weeks. In chronic trauma or late evaluation of the effects of trauma, the development of fibrosis does not hinder nerve imaging because most classes of fibrosis have very different image characteristics than nerve - no long T2 low protein water component to contend with.

Conspicuity and reconstructions

One important aspect of MR Neurography is to use MRI pulse sequences and acquisition strategies that tend to make nerve image intensity brighter than that of immediately surrounding tissues. When this is achieved, it greatly aids the process of generating three dimensional projection images as well as multi-planar reformatted images. This process often helps in the appreciation of overall nerve course and of variations of the various types of other image findings as they vary along the length of a nerve. Among the 5,000 cases evaluated, more than 99% were susceptible to 3D analysis. Findings in the 3D reports revealed additional information not appreciated in 2D analysis in 28% of cases The greatest amount of additional diagnostic information in these analyses occurred in the brachial plexus cases. Because of the significant incremental amount of clinical information provided by this type of analysis and the susceptibility of most studies to this, these were considered essential aspects of the diagnostic interpretation process in this group.

Multi-planar reformat and Maximum Intensity Projection (MIP) reconstructions were also important in limiting artifactual variations in nerve image intensity that can occur from partial volume averaging – this means that when a given sampled voxel is partially filled with nerve and partially filled with an adjacent low intensity tissue, the resulting pixel on the image will appear to show low intensity nerve. Reconstruction techniques such as multi-planar reformats in linear planes allow the reading clinicians to readily assess this sort of issue. Curved reformats made along a “nerve course plane”

drawn along the main nerve axis by a technologist or radiologist reduce the accuracy of the spatial information but provide for optimal reduction of image intensity averaging effects.

Image Findings in Brachial Plexus Studies

MR Neurography proved effective for identifying the presence of a variety of types of abnormalities in brachial plexus studies. These include distortions of the course of the proximal elements at the scalene triangle (Fig 6, Figs 7A-D), fibrous band entrapments affecting C8 and T1 spinal nerve and the lower trunk of the brachial plexus (Fig 7F), gross distortions of the mid-plexus (Figs 7G & 7H), hyperintensity consistent with nerve irritation at the level of the first rib (Fig 6), and distal plexus hyperintensity.

In most peripheral nerve studies it has proven useful for identifying areas of hyperintensity consistent with nerve irritation by a comparison of results from following serial nerve cross sections oriented to be perpendicular to the principal long axis of nerves to images taken to be more or less parallel to the long axis. In nerve-perpendicular images, the fascicle pattern can generally be observed. This will demonstrate expansion of the fascicle compartment at the expense of the interfascicular compartment at areas of focal hyperintensity. The nerve-parallel images can provide a linear overview. In general

effective interpretation of nerve parallel images depends on the ability of the MR Neurography imaging sequence to make the nerve brighter than surrounding tissues. In this fashion the nerve image plane can be adjusted by multi-planar reformatting or the nerve can be assembled by maximum intensity projection. If this is not done, then partial volume effects at the edges of nerves can lead to artifactual appearance of variation of image intensity within an image. In the brachial plexus, multi-planar reformatting is usually sufficient to generate a series of images that can reliably confirm the existence of a focal change in nerve image intensity. This is aided by positioning the patient in the scanner in a way that tends to straighten the plexus. When a change in the fascicle pattern shows increased intensity in the nerve perpendicular views that matches to a change seen in nerve parallel views, there can be a very high level of confidence about the clinical reality of nerve edema at the location that appears abnormal in the image.

MR Neurography in the Pelvis

The use of MR Neurography has revolutionized neurologic diagnosis in the pelvis . Although sciatic pathologies have been an important part of the advance, the ability of MR Neurography to track other nerve elements in the pelvis has gone a long way to resolving what had been a troublesome “black box.”

In the face, neck arm and hand patients tend to be very effective in identifying the location of pain, numbness and dysfunction. Physical exam is straightforward and well understood by many clinicians. Electrodiagnostic studies are readily applied. In the pelvis, the situation is quite different. Although the sciatic nerve in the leg poses similar accessibility to what the clinician experiences in the upper body, there has been great difficulty in applying physical exam, imaging, and electrodiagnostics in the pelvis. Further, patients often have a great difficulty explaining the location of pains. It is common for low buttock pain to be described as “back pain” while patients readily distinguish between shoulder and neck. The term “groin” pain could refer to problems involving the femoral nerve, ilioinguinal nerve, genitofemoral nerve, pudendal nerve, obturator nerve or nerve to the obturator internus among others.

The ability to reliably locate all of these nerve elements in MR Neurography images greatly aids physical exam. The ability of Open MR guided injections to distinguish superior gluteal nerve, inferior gluteal nerve, posterior femoral cutaneous nerve, cluneal nerve (superior, middle, inferior), nerve to obturator internus, nerve to quadratus femoris has also supplemented the role of MR Neurography for identifying pathology in these nerves. Simply by clarification of the nerve course anatomy, it has also greatly enhanced the efficacy of physical exam and clarified the meaning of a variety of new types of physical exam maneuvers.

With regard to lower extremity radiculopathy, it has made it convenient to determine distinctions by imaging that help locate impingements in spinal foramina, at the distal foramen, at lateral marginal osteophytes several centimeters distal to the foramen (Fig 8), in the lumbo-sacral plexus, on the medial aspect of the piriformis muscle (Fig 9), in association with division of the nerve by the piriformis muscle (Fig 10), at the ischial margin, at the tendon of the obturator internus, at the distal ischial tunnel on the lateral aspect of the ischial tuberosity and at various locations in the thigh. Because MR Neurography is a very sensitive test, a completely negative MRN (Fig 9) is often very useful, just as a completely normal lumbar MRI can be - in both cases, the definitively negative study can substantively change the direction of further diagnostic efforts.

Reliable identification of anatomical variants of the sciatic nerve now plays a critical role in improving the safety of surgeries for the release of pelvic sciatic nerve entrapment. Isolated section of a single piriformis segment in patients with a split nerve passing through a split muscle can cause nerve compromise after surgery if this condition is not detected in advance (Fig 11).

Identification of the presence or absence of pudendal nerve hyperintensity consistent with nerve irritation in the Alcock canal (Fig 12) along the medial aspect of the obturator internus muscle or at the rectal branch of the pudendal nerve proximal to its entrance to the Alcock canal (Fig 13) has also been quite useful clinically .

Imaging of the complete course of the L4 spinal nerve as it progresses into the femoral nerve has made it possible to search for abnormalities along the intra-abdominal and intra-pelvic course that were previously almost impossible to diagnose. Identification of abnormalities along the ilio-inguinal and genitofemoral nerves are similarly greatly aided by MR Neurography.

Nerve Imaging for Distal Entrapments

Distal entrapments including less common problems such as posterior interosseous nerve entrapment of the distal radial nerve as well as common issues such as peroneal nerve entrapment at or above the fibular head, tarsal tunnel syndrome, cubital tunnel syndrome and carpal tunnel syndrome benefit from MR Neurography imaging when physical exam or electrodiagnostic studies show that locations other than the most routine sites may be involved. For instance, median nerve entrapment in the distal forearm can lead to failure of treatment if only the flexor retinaculum is addressed. Ulnar entrapment in Guyon's canal, and proximal peroneal nerve entrapments along the tendon of the biceps femoris just distal to the sciatic bifurcation are other specialized issues that can best be investigated by imaging. Electrodiagnostics can be misleading if they are done with the assumption that abnormalities in certain regions (e.g. the median nerve in

the distal forearm) will always be at the flexor retinaculum – particularly if uncomfortable and time consuming “inching” studies are not done.

Clinical Outcomes and MR Neurography

The evidence for clinical utility for MR Neurography has been evaluated with two different types of outcome studies. Firstly, it has been compared with electrodiagnostic studies in the well defined environment of assessing median nerve compressions at the wrist. In this setting, evaluating 120 patients, MR Neurography has proven to be as effective or slightly better than electrodiagnostics for predicting which patients will have good surgical outcome from carpal tunnel decompression. Secondly, a different paradigm has been applied using Class A study methodology for evaluating the utility of MR Neurography for positively affecting patient outcomes in proximal sciatic entrapment - a condition for which there is no gold standard method. In this study evaluating 239 patients, use of MR Neurography resulted in a strongly significant improvement in success for treating patients with sciatica who had either negative diagnostics or failure of treatment when managed by information from standard diagnostics alone. In these studies, image interpretation was carried out by neuroradiologists blinded to outcome results.

II. Diffusion Tensor Imaging

From the earliest report on the use of DTI to image neural pathology , it has been clear that this technique has great potential for use in detecting inflammatory brain conditions. It is also proving to be promising for evaluation of stroke, dementia and diffuse axonal head injury and to aid in surgical navigation in brain tumor resections. It is also being explored for evaluation of myelopathy in the cervical spinal cord. It is very demanding from the point of view of motion suppression, but increasing clinician experience with the special requirements is leading to steady advances in establishing the utility of the technique.

Physical Basis

Nuclear magnetic resonance generally depends on using a radiofrequency stimulation to push energy into a group of nuclei and then using an antenna to detect the decay of the stimulated signal. For a given type of atomic nucleus - such as the single proton nucleus of hydrogen atoms, there is a rate of nuclear spin rate or frequency that is related to any magnetic field applied to the nucleus according to a physical relationship we call the gyromagnetic ratio. This means that, for instance, in a 4.7 Tesla magnetic field, hydrogen nuclei will be aligned with the direction of the main magnetic field and have a natural spin rate (resonant frequency) of 200 MegaHertz (MHz), in a 1.5 Tesla magnet, the spin rate will be 64 MHz, etc. So, for a given magnet field strength, we know

the resonant frequency for hydrogen nuclei and can pump in a pulse of radiofrequency energy at that resonant frequency. This causes most of the protons in the volume to spin in phase with each other. They will then emit a radiosignal at that frequency that can be detected when the incoming stimulus pulse is turned off. With elapse of time over tens and hundreds of milliseconds, the protons will gradually lose their coherent behavior - some will spin a little faster, some a little slower, and the return signal will gradually decay away.

When we measure the T1 and T2 decay rates, we are observing the effects of the spins interacting with their surroundings or "matrix" - for instance, a little bit of iron in the tissue will perturb the magnetic environment to a variable degree (T1 decay) and will also see the effects of the protons interacting with each other (spin-spin or T2 decay). Because these decays occur at differing rates in different tissues we can see contrast between tissues that we can express as grey or white in an image of a volume that we are measuring.

In Magnetic Resonance Imaging, we use magnetic gradients in the three planes to assign a slightly different field strength to each location in the tissue volume. For instance, in the very center, the field strength could be 4.7 Tesla, but a little to the right it would be 4.7001 Tesla and a little to the left it would be 4.699 Tesla. The protons on the right now spin at 200.001 MHz and the protons on the left spin at 199.99 MHz. In this fashion we can assign a unique field strength and therefore a unique frequency to each

voxel (3D pixel) in our imaging volume and we can "listen" individually to the decay rate in each individual volume in the tissue. The entire process is done with a mixed complex of frequencies and a Fourier Transform is used to sort them all out.

In diffusion imaging, we rely on a different property of tissue to establish an entirely different source of information from spin decay. A pulsed "diffusion" magnetic gradient is applied so that as water molecules diffuse to different locations in a tissue, their spins dephase - because a group of water molecules that started out next to each other in a single field strength, now find themselves in different field strengths and so they have different spin rates and so the spins dephase from each other resulting in signal decay. Water molecules in some tissues diffuse equally in all directions (isotropic diffusion), but in nerves and nerve tracts, diffusion takes place preferentially along the long axis of the nerve tract (anisotropic diffusion) (See figure 14). If a magnetic gradient is directed perpendicular to the direction of a nerve or tract, the water diffusing in the nerve will tend to remain in the same strength region of the gradient and will show relatively little decay from diffusion - gradually becoming brighter relative to the tissue around it. However, if the gradient is then oriented parallel to the direction of the nerve, then the anisotropically diffusing water molecules will tend to move up and down the gradient more rapidly when compared to isotropically diffusing water molecules and so will actually experience a more rapid signal decay - making the nerve tend to go dark relative to other tissues around it.

However, what if the nerve or tract takes a curved course? How do we get the diffusion gradient to be perpendicular or parallel to it? This was the essence of the problem, but the solution comes from very simple mathematical geometry. In essence, if we can determine the degree of anisotropy in each voxel relative to the three principle directional axes, we can provide an estimate of the true dominant direction of anisotropy inside the three dimensional space of that voxel. The direction, whether in two or three dimensions is a vector, however - as will be explained below - we need a more elaborate data structure called a "tensor" in order to fully describe the anisotropy data. Isolated diffusion measurements provide an orientation but not a direction (e.g. the anisotropy goes up and down the z-axis) - it turns out that to fill out the nine elements of the matrix that describes a tensor in three dimensional space we need at least six measurements.

In standard diffusion weighted imaging, we want to know the total amount of anisotropy vs isotropy within a given voxel when viewed from a particular direction. For DTI, we want to know both the true magnitude and the true three dimensional direction of the anisotropy in each voxel independent of the angle from which we view the voxel. This information is used in two different ways - we can make an image slice in which the relative amount of anisotropy is described as the Fractional Anisotropy (FA) which more or less determines how bright a voxel will be and uses a standard set of colors to depict some of the information about the orientation of the fiber tracts. This results in cross

sections showing some of the information about bulk orientation of white matter tracts in regions of the brain.

The other way to use the information is for tractography. Here, various mathematical algorithms are applied to generate linear tracts in three dimensions that represent the course of bundles of axons in the white matter of the brain or of nerve fibers in peripheral nerve (see Fig 15).

From one point of view the development of DTI and tractography was hindered for many years by a mathematical model deriving from Basser and LeBihan due to the "elipsoid" formalism that takes a different approach to the analysis than in the original vector and tensor model from Filler and Richards that underlies modern tractography:

The equations used for the first DTI image are as follows:

(1) $(\text{Vector length})^2 = BX^2 + BY^2 + BZ^2$

(2a) Diffusion vector angle between BX & BY = arctan (BY/BX)

(2b) Diffusion vector angle between BX & BZ = arctan (BX/BZ)

(2c) Diffusion vector angle between BY & BZ = arctan (BY/BZ)

The first of these basic equations establish a tensor length analogous to what is now called the Fractional Anisotropy (B is equivalent to the decay time measured in each of the three axes assessed in three separate measurements, X

then Y then Z). This vector length calculation has the important effect of making the measurement of the amount of anisotropy in a given voxel independent of the orientation of the anisotropy relative to the orientation of the gradients applied. This made it possible to make, for the first time, a valid image showing the degree of anisotropy in all parts of each image slice. Previously - in a standard diffusion imaging model - a given tract would be bright or dark depending on its orientation in a given voxel even if it was highly anisotropic at that location.

The second set of equations allows us to take three looks at our voxel - each seeing it in two dimensions. It uses the arctangent function to measure the angle between the neural tract and the gradient axis direction that is in denominator of the equation. If BY is 0.1 and BX is nearly 1.0, then the arctangent of BY/BX will be about 5 degrees. When the measure is equal in two directions (Y = 0.5 and X = 0.5), the arctangent is 45 degrees.

Because of the vector length and the arctangent function, we can correctly interpret a voxel in which all three angles of measurement are equal. It does not describe a sphere nor does it describe an isotropic voxel. We know it has length and is oriented at 45 degrees to the reference frame - a line along the diagonal of the cube. We can also depict the arctangent value in successive voxels to see

coherence in the angle of direction from voxel to voxel as we progress along a neural tract.

However, for reasons described below, we can only use this sort of three axis data for DTI in particular limited tractographic tasks where we can use information from previously known anatomy to guide the process. For this reason Filler and Howe also proposed use of a number of gradient acquisitions in a larger number of arbitrary directions which could then be used to establish the true direction of a neural tract independent of any fixed known axis.

Basser and LeBihan proposed that each voxel be viewed as containing an elipsoid that needed to be defined in shape from six different gradient measurements rather than just three. Although it is true that the thickness of the elipsoid encodes relevant information about the fine structure inside each voxel, the practical finding has been that only the fractional anisotropy and the primary eigenvector - the length and direction of the long axis of each elipsoid - has been required. This is because the tensor model as originally described by Filler, Howe and Richards models axons. In their fundamental anatomy, these are linear structures and any analysis that turns them into series of complexly shaped and directed elipsoids can actually obscure the underlying biology and biophysics.

Collecting images that accurately describe the elipsoids is still a usable formalism but the measurements of the thickness and equatorial orientation of the "jellybean" have so far proven to have little use in tractography. The ellipsoid representation makes more sense in some areas of physics such as magnetic or electric field studies, but has no clear biological correlate in neural tract tracing.

As discussed below there is an equally usable formalism that is closer to the anatomy of the axons and neural tracts. In any case, the data processing will continue to advance in complexity as dozens or even hundreds of different gradient axes are sampled - posing significant technical challenge in MRI well into the foreseeable future.

Tensors and Vectors For MR Imaging

At first glance, it might seem that if we measure diffusion in three directions that are the orthogonal x, y an z axes in a Cartesian 3D space, then we will be able to know the length and direction of a vector that we can use to support tractography and FA analyses (see Figure 16). The problem is that diffusion measurements in a given orientation do not distinguish which direction the water molecules are moving along the measured axis. In fact, the molecules do move both proximally and distally along the axon, but are only restricted in that that they tend to move along the long axis of the axon rather than freely in any direction.

To understand the implications of this, you can consider a three dimensional coordinate system such as we see in figure 17-I. When we provide a measurement showing prolonged decay of 100 milliseconds along the x-axis (axial orientation), we must draw this as a line running from +50 to -50. Now we can measure in the y-axis (coronal) and lets use 100 milliseconds again - that is it seems bright in the second axis as well. Returning to our drawing, we draw the line from +50 to -50 on the y-axis.

If we look for an axon line that would meet this description, we get four different options on the vectors that might tell us where the axon might be. When we take a third measure - this time in the z-axis (sagittal) and again get a result of 100 milliseconds, we have to draw a third line - this time from +50 to -50 on the z-axis. We now have eight different possible solutions - eight different diagonal vector lines running through each of the eight octants of three dimensional space in our voxel.

We can now start to get some help in figuring out the real tract direction if we measure in a fourth axis and then a fifth axis, each oriented along one of the diagonals as shown in figure 17-II. When this comes back as 3 milliseconds, we know we can throw out any of the vectors that had a significant apparent length in the four octants that our plane passes through. A sixth measurement is then made along one of the remaining diagonals which - in this example - comes back as 4 milliseconds (see Figure 17-III). This eliminated two more octants and leaves only one possible solution.

If, instead, the sixth measurement had been along the diagonal with the actual neural tract, it would measure out around 140 milliseconds - which happens to follow the Pythagorean theorem relative to our other positive measurements (hypotenuse of a right triangle equals the square root of the of the sum of the squares of the two sides - $(100)^2 + (100)^2 = (140)^2$). With this information, we can be confident that one pair of vectors represents the line across our voxel that is the correct source of the signal.

The fact that six measurement will always solve the problem seems puzzling, but we can gain confidence by understanding that there is a basis for this in mathematical geometry. The information comes from a special area called tensor analysis.

It is not true that a tensor is just a three dimensional vector. Tensors are defined on complex mathematical grounds and do not necessarily have any simple geometric equivalent the physician or biologist can readily rely on to support an understanding of them. Einstein struggled with aspects of tensor theory for a few years before he was able to understand them well enough to use them as the basis for his theory of relativity. To make matters worse, there a number of different ways that tensors can be explained and defined - some deriving from formal modern mathematics, some from physics, some from engineering.

For the purpose of understanding diffusion tensor imaging, however, there is a reasonably accessible approach. A scalar is a simple number. A vector has a length and a

direction. A scalar can also be described as a tensor of rank 0. A vector can also be described as a tensor of rank 1.

In the example above, we showed a number of vectors that were bound to the zero point of a Cartesian coordinate system. It is readily apparent that these vectors were three dimensional objects. Each vector could be "expanded" for its description. Expansion is a mathematical term that means we could give a scalar on each of the three axes and use these three numbers to uniquely describe the vector (see figure 16). As we saw in our example - three measurements might be enough to describe a vector, but if we don't know the sign or direction on each axis, then this clearly is not enough information to describe the direction of an axon or neural tract as it traverses our MRI voxel.

For tractography, we need to use some kind of tensor of rank 2. There are a number of different mathematical constructs that are rank 2 tensors. One thing they all share in common is that they can be fully described by nine measurements - often written out in a 3 by 3 matrix. However, since six measurements fully describe our neural tract you might expect that there is some special type of tensor we need to focus on.

The correct construct is called a dyad. This is a structure that has a scalar quantity and two directions. Fortunately for biologists and physicians, it is acceptable to conceive of a dyad as being made up of two vectors. Even more specifically, what we need for our neural tract is a type of dyad called an anti-symmetric dyad. This is a dyad in which the two vectors are identical in length (symmetric), but have exactly opposite directions.

One consequence of the anti-symmetry is that we don't need all nine measurements to fully describe the dyad. Three of the measurements can be dispensed with because of the symmetric nature of the mathematical structure.

Because an anti-symmetric dyad is a special case of a tensor of second rank, we can take advantage of a wide expanse of mathematical formulations for assembling and manipulating the data we collect. However, it is not true that our diffusion tensor measurements form a classical tensor field.

One of the original ideas behind tensor math was the problem in physics and engineering that arises when we have a stress applied to a surface of a cube. We consider that the cube is placed under strain and is deformed by the tension of the applied force. However, the strain will differ from place to place in the solid depending on the material it is made of and the way that the force of the stress is being applied. A tensor field might be used to generate force vectors for each unit volume of the cube in a predictable mathematical progression.

However in the diffusion tensor data set in clinical MRI, the field of tensors in the brain (for instance) is determined by anatomy and really cannot be arrived at by any complex mathematical formula. We can generate tractographic atlas data to use in algorithms to help guide the tractographic process, however, for the most part, the preference has been to allow the tractographic process to proceed from the data collected for each voxel in the imaged area.

Tractography is done in a wide variety of ways, but there are two main classes of approaches to the problem. In one group of methods, we more or less follow from one dyadic line to the next using various seeds as starting points. In the other group of methods we lay out the field of dyadic tensor lines and try to allow a line to find the lowest energy course (the path of least resistance) through the thicket of dyads.

Future Challenges

An additional challenge for tractography derives from the fact that diffusion imaging in general and diffusion tensor imaging especially, are extremely sensitive to motion. This is because we are trying to measure the motion of water molecules due to diffusion. At a very fine level, brain pulsations due to the arterial pulse and respiratory effects on the venous pressure - along with bulk movements from respiration, can only be suppressed by extraordinarily rapid imaging - images requiring a fraction of a second to acquire.

Even with complete suppression of motion, brain tractography is limited by the problem of fiber tracts in differing directions passing through each other. Many of these conflicts can be resolved with increasingly fine spatial resolution - so that a given voxel tends to contain fascicles mostly with a single direction. However, very fine spatial resolution requires very high signal to noise performance. This can be accomplished with long repetitive scans in high field magnets (3Tesla), but the very fast echo planar scans

used to suppress motion and acquire multiple gradient axes tend to lose ground on signal strength and spatial resolution.

There are a few situations in which a limited number of gradient orientations can be sufficient. This is the case if we use an Atlas or a non-diffusion nerve image in peripheral nerve tractography as a guide to make decisions about which axes to accept and which to ignore. Another simple method proposed by Kinosada is to use one or two gradient acquisitions - to generate bright spots in cross sectional images. We then apply maximum intensity projection methods to look through a stack of these images in order to convert the two dimensional data to three dimensional tractographic images - much like the methodology is some forms of MR angiography. This is more likely to be effective with peripheral nerve since it has low resolving power for diverging tracts along complex courses such as we find more frequently in the brain.

In any case, the compromise of using the single primary eigenvector or the equivalent anti-symmetric dyad and dispensing with full use of the additional information in the ellipsoid, has made it possible to carry out good tractography in 1.5 Tesla MRI scanners on most patients. The power of Diffusion Tensor Imaging is therefore now starting to be revealed.

Clinical Utility of DTI

A critical aspect to keep in mind is that in T2 MR Neurography, the nerve anatomy becomes progressively more clear and detailed as the pathology becomes more severe. The opposite is true of DTI. Any significant irritative or ischemic abnormality tends to decrease the anisotropy and therefore to make the involved neural tracts disappear. Although this means that DTI tractography studies can be read for tract 'drop out' as a sign of pathology, it also means that tractography must be assessed very carefully when it is relied on to demarcate tract borders near tumors or other irritative lesions.

Although simple diffusion weighting (DWI) is very useful for identifying cerebral infarctions, DTI has greatly expanded the clinical utility of diffusion decay information. The key difference between DWI and DTI is reliance on the Apparent Diffusion Coefficient (ADC) in DWI versus the Fractional Anisotropy (FA) in DTI. Simply put, the ADC provides a single "scalar" number that estimates the relative degree of anisotropy vs. isotropy in a given voxel. The estimate is flawed because it eliminates anisotropy signal arising from differences in orientation of the direction of diffusion that occur between the axons in the volume and the arbitrarily chosen imaging planes. The FA, on the other hand measures the anisotropy in each voxel in a way that closely approximates the true length of the tensor in each voxel, whatever direction it is pointing in.

The beneficial effect on the quality of diffusion data that results from use of FA as opposed to ADC is already clear from the first few formal outcome studies to emerge that formally evaluate the clinical utility of the FA measurement. In a study of 17 patients comparing ADC and FA measurements in white matter tracts adjacent to spontaneous intracerebral hemorrhage, the FA provided a statistically significant prediction of outcome, while ADC did not. In a longitudinal study with repeat imaging and FA analysis in 23 patients with traumatic brain injury, increase in FA was highly correlated with increase in Glasgow outcome score during recovery and that most of this correlation derived from the principal eigenvalue parallel to the main direction of the axons in a given voxel.

The use of tractography in image segmentation for tumor resection planning has now also been formally evaluated in a randomized controlled, prospective trial involving 238 patients, that compared success of gross total resection, Karnofsky performance at 6 months, and survival from high grade gliomas using neuronavigation guidance from DTI tractography versus neuronavigation from standard MRI. This study showed statistically significant improvement in these measures when DTI tractography was used, resulting in a 43% reduction in risk of death in the hazard risk time period evaluated.

Conclusions

At this point, it is clear that when the precise location of a peripheral nerve lesion cannot be determined externally then nerve imaging should be carried out. Since MR Neurography demonstrates pathology as well as anatomy due to its view into the intrinsic signal from the endoneurial fluid it should be the method of choice unless there is some overwhelming reason to desire not to know the available information.

DTI imaging provides increased sensitivity for CNS pathology relative to other MR based imaging techniques. Because fractional anisotropy encodes directional and functional information not captured by other techniques, it has higher information content regarding pathology affecting both structure and membrane stability. It appears to be indicated for diagnostic and prognostic information as well as for tracking recovery in the setting of ischemic, traumatic, inflammatory, infectious, and degenerative disease - particularly when asymmetric pathology is suspected that will allow comparison between an ipsilateral affected side and contralateral unaffected side.

Like spine imaging, neurographic and tractographic imaging can provide false positive findings, however, these are often very specific anatomically and can be considered and tested for clinical relevance.

The technical aspects of imaging hardware that will improve MR Neurography in the future include larger areas of excellent magnetic field homogeneity - this will allow for large field of view studies with uniform fat suppression and image quality throughout the larger image volumes. Improvements in antenna coil technology will also tend to

improve signal to noise. Use of black blood contrast agents such as ferrite agents could be applied for visualization of very small nerves where the anatomical distinction from very small vessels is unreliable.

For diffusion based methods such as DTI, even the vibration of the scanner caused by the interactions between the gradient coils and the main magnetic field have become a significant problem limiting spatial resolution. This is the interaction that causes the typical knocking sound - which can rise to a deafening level when high fields, powerful, fast rising gradients, and very rapid pulse sequences are deployed. The solutions here include design of magnets with inertially resistant gradient coils that provide physical dampening of vibration along with advances of design of balancing gradients that cancel the physical and mechanical effects of the magnetic interaction. The resulting improvement in spatial resolution and signal strength will be necessary to help to resolve brain regions where fiber bundles pass through each other in different directions or where they diverge slowly.

The introduction of imaging techniques capable of demonstrating the intrinsic signal of nerve as well as of preserving and displaying structural linear properties of neural tissue in general is progressively transforming all of neuro-imaging even as it transforms our approach to diagnosis, treatment planning and surgical access. The next ten years will be an extremely exciting period for the various forms of neural tractography. It is reasonably expected that there will be a logarithmic expansion of the

utilization of these techniques so that more than 5 million such imaging studies will probably be performed in the next ten years.

Many of the fundamental obstacles have been overcome and the advance of the power of imaging equipment and post-processing technology will similarly help drive these methods to the forefront of neurology and neurosurgery.

Figures & Legends

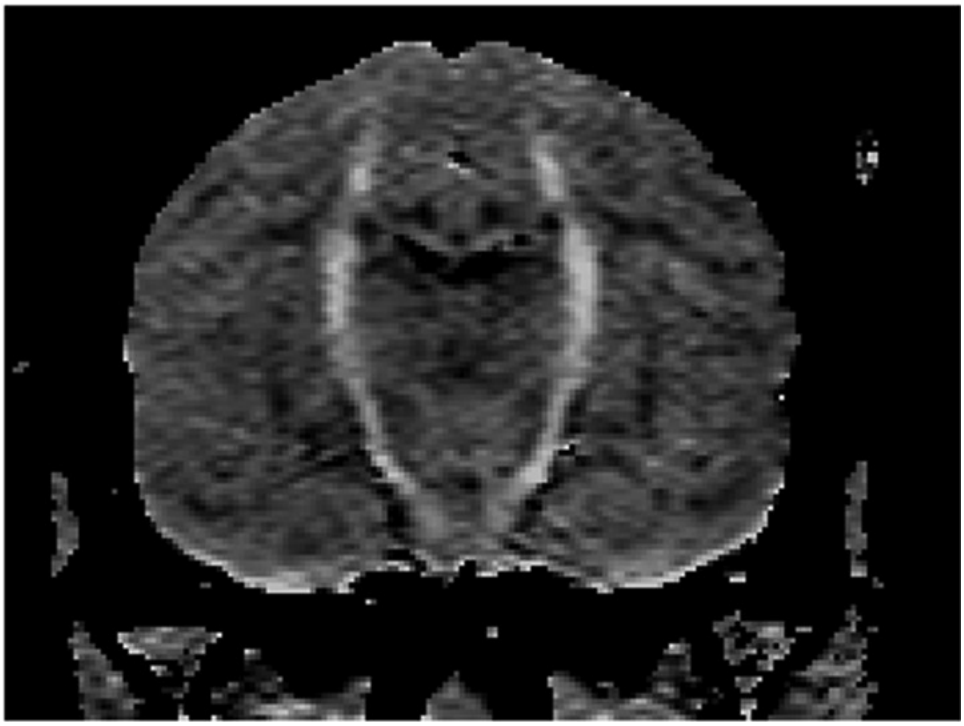

Figure 1 – The first Diffusion Tensor Imaging case. This image is primarily the work of Todd Richards and shows the use of spatial diffusion information to highlight a neural tract curving through brain. This is the brain of a long-tailed macaque monkey (*Macaca fascicularis*) imaged as part of an effort to improve the sensitivity of MRI for the early detection of encephalomyelitis. Reproduced from: Filler AG, Tsuruda JS, Richards TL, Howe FA: *Images, apparatus, algorithms and methods.* GB 9216383, UK Patent Office, 1992 and also: Filler AG, Tsuruda JS, Richards TL, Howe FA: *Image Neurography and Diffusion Anisotropy Imaging.* US 5,560,360, Unites States Patent Office, 1993 .

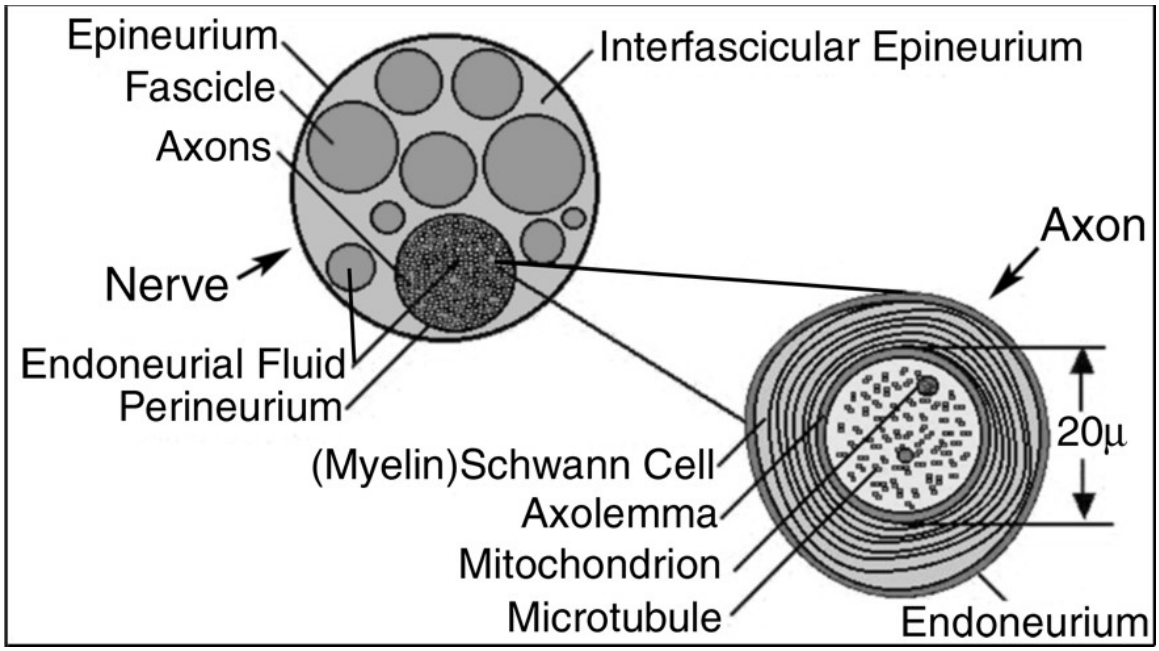

Figure 2 - Nerve water compartments. MR pulse sequences can be optimized to detect water signal arising in one of several compartments. Important nerve water components with unique characteristics for MRI include the endoneurial fluid, axoplasmic water, organelle water and myelin associated water.

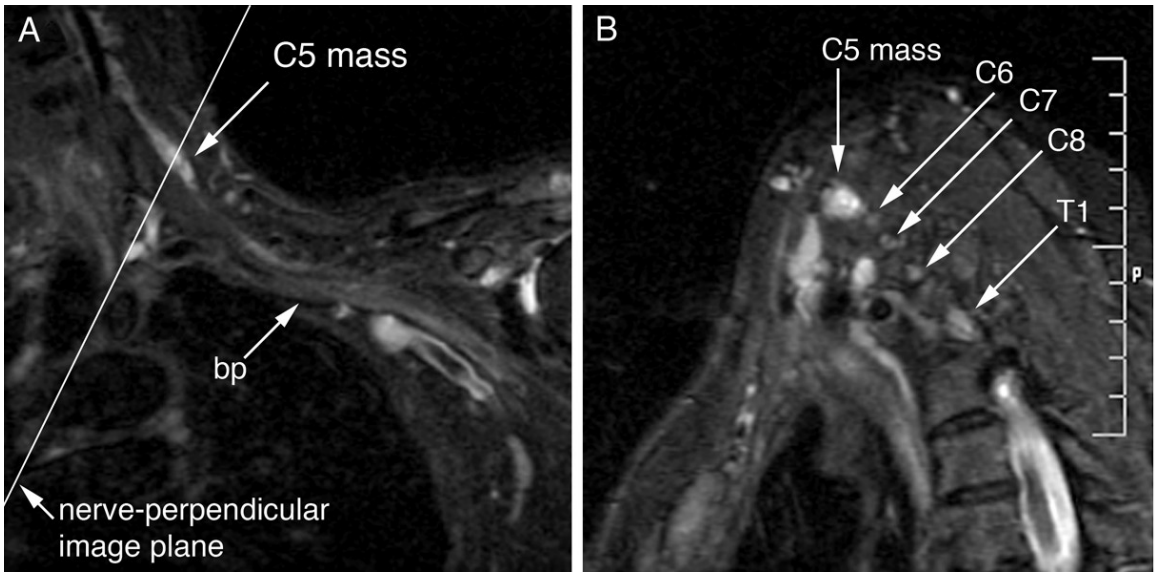

Figure 3 – Relations of a small C5 mass to brachial plexus elements. In many cases, by collecting images in planes that are perpendicular to the main longitudinal axis of the nerve elements of interest, it is possible to obtain extremely specific information about the location of a mass within the brachial plexus.

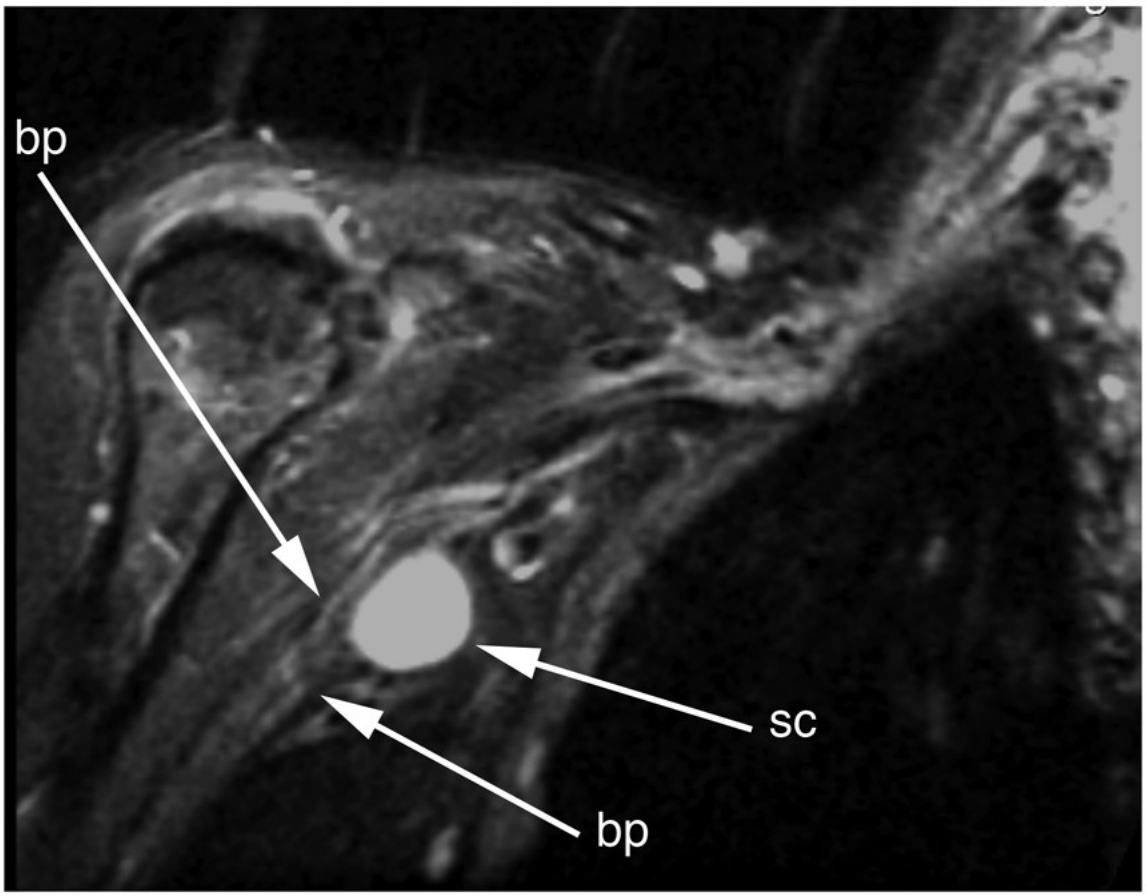

Figure 4 – Relations of brachial plexus elements to an axillary mass. Although schwannomas can be detected by various techniques, it is extremely valuable for the surgeon to have a method of determining the position of the nerve elements relative to the position of the mass. Bp – brachial plexus, sc – schwannoma.

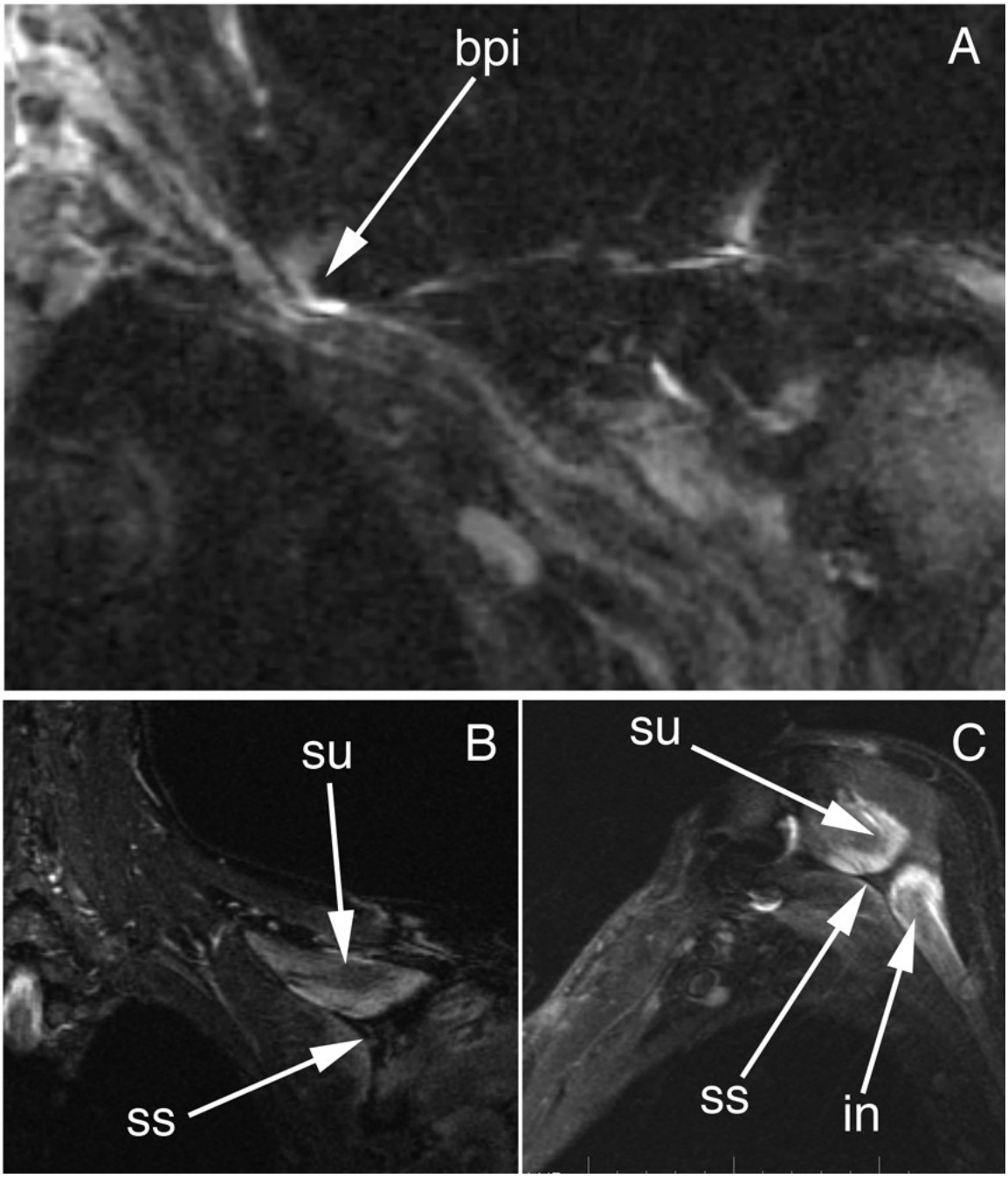

Figure 5 – Upper trunk brachial plexus injury with denervation of C5 muscles. A) There is an apparent discontinuity of the C5 component of the upper trunk. The C6

component is swollen upstream of the injury and sharply narrowed and hyperintense. B) Coronal view and C) nerve perpendicular view showing severe denervation changes in supraspinatus and infraspinatus muscles. Bpi – brachial plexus injury, su – supraspinatus, in – infraspinatus, ss – scapular spine.

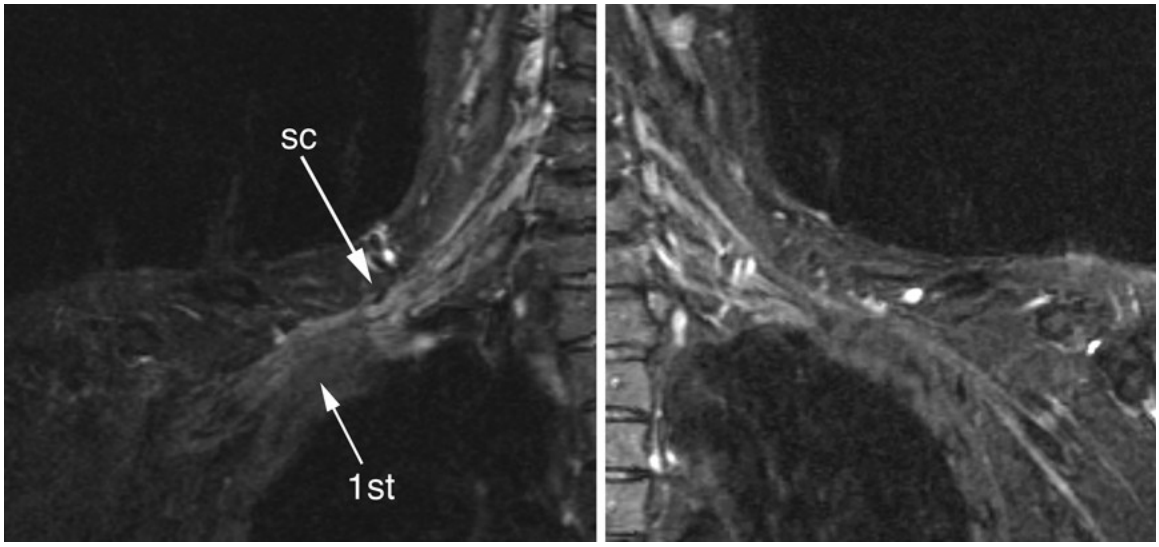

Figure 6 – Right and left side comparison of a patient suffering from right sided thoracic outlet syndrome. The image demonstrates several types of abnormality detectable by MR Neurography relative to the normal side. There is increased caliber and image intensity of nerve elements on the left and two sites of impingement. A sharp focal downward distortion at the lateral border of the scalene triangle and then a gently sloped upward distortion over the first rib. Sc – scalene border, 1st – first rib.

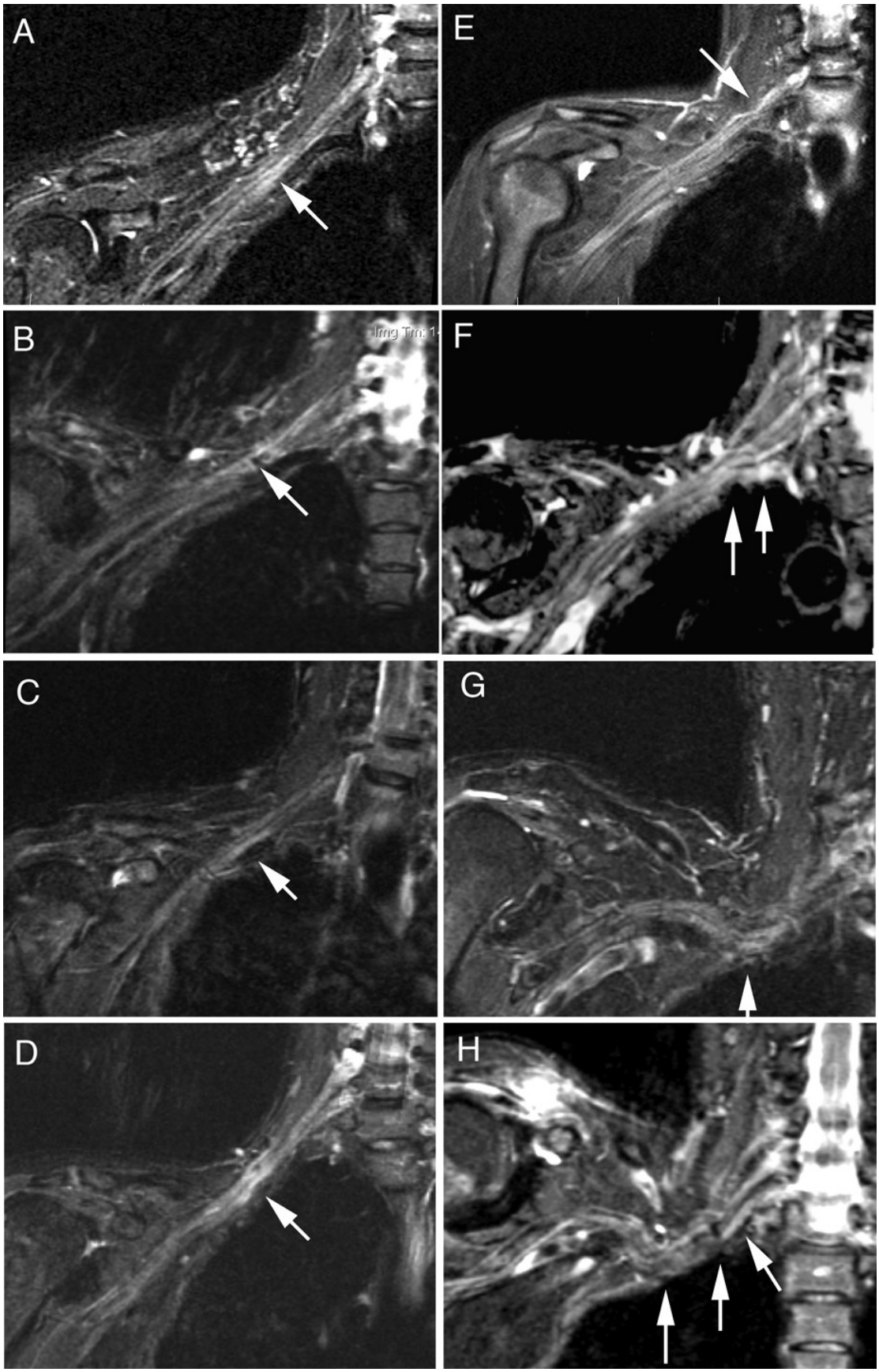

Figure 7 – Varying degrees of severity of brachial plexus entrapment in thoracic outlet syndromes. A) Linear plexus with short segment of mild hyperintensity consistent with nerve irritative changes near the later border of the scalene triangle; B) Evidence of more restrictive fibrosis associated with narrowing and brightening of plexus elements near the scalene border – note linear plexus despite elevated shoulder; C) Short segment of marked hyperintensity with slight swelling; D) Severe multiple element abnormality with narrowed and swollen segments, and marked hyperintensity; E) Linear normal plexus with isolated focal impingement of C5 spinal nerve, just proximal to the scalene triangle; F) Fibrous band causing sharp downward distortion of mid and lower trunk proximal to scalene triangle, with second sharp upward distortion of lower trunk near scalene insertion at the first rib; G) Moderate restrictive impingement of plexus at scalene triangle causing generalized distortion of the course of the plexus with short segment of focal hyperintensity; H) Patient presenting with severe pain, numbness and weakness from progressive thoracic outlet syndrome – multiple points of sharp nerve course distortion with edema and hyperintensity affecting multiple brachial plexus elements.

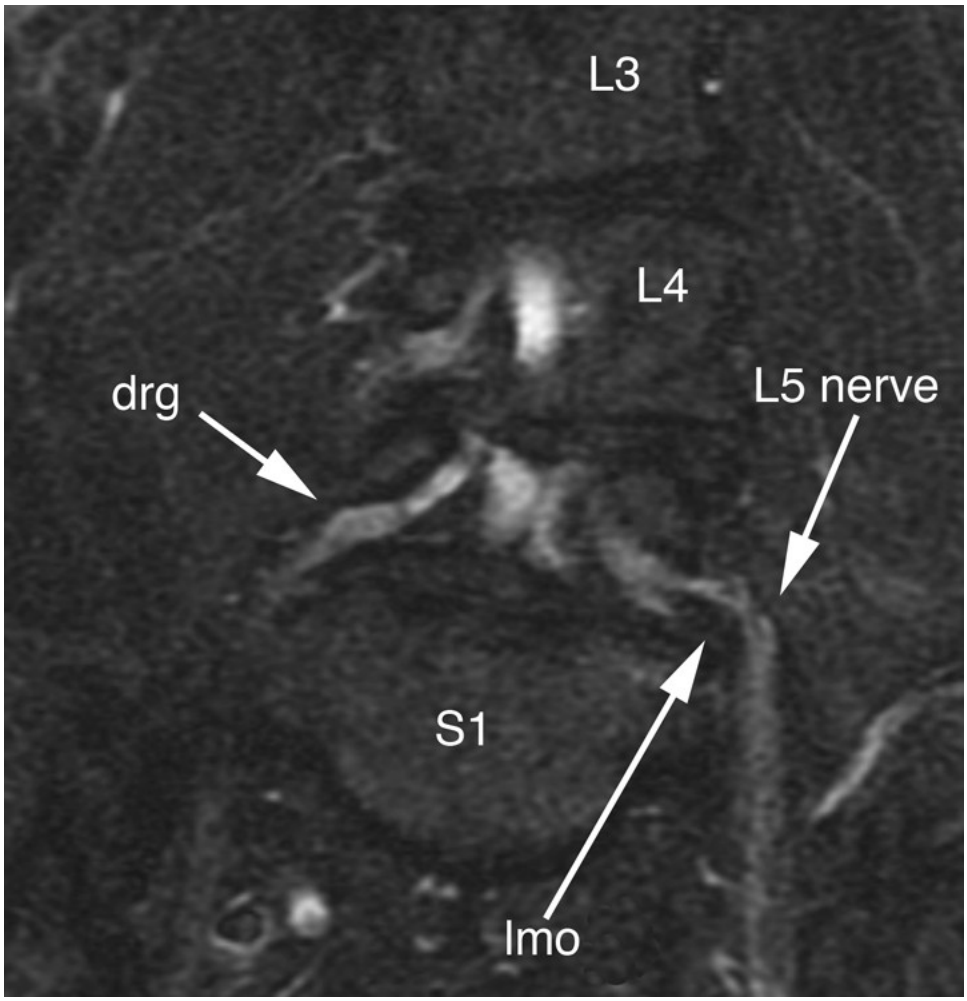

Figure 8 – Extraforaminal impingement of descending L5 spinal nerve by lateral marginal osteophyte distal to the foramen. Drg – dorsal root ganglion, lmo – lateral marginal osteophyte.

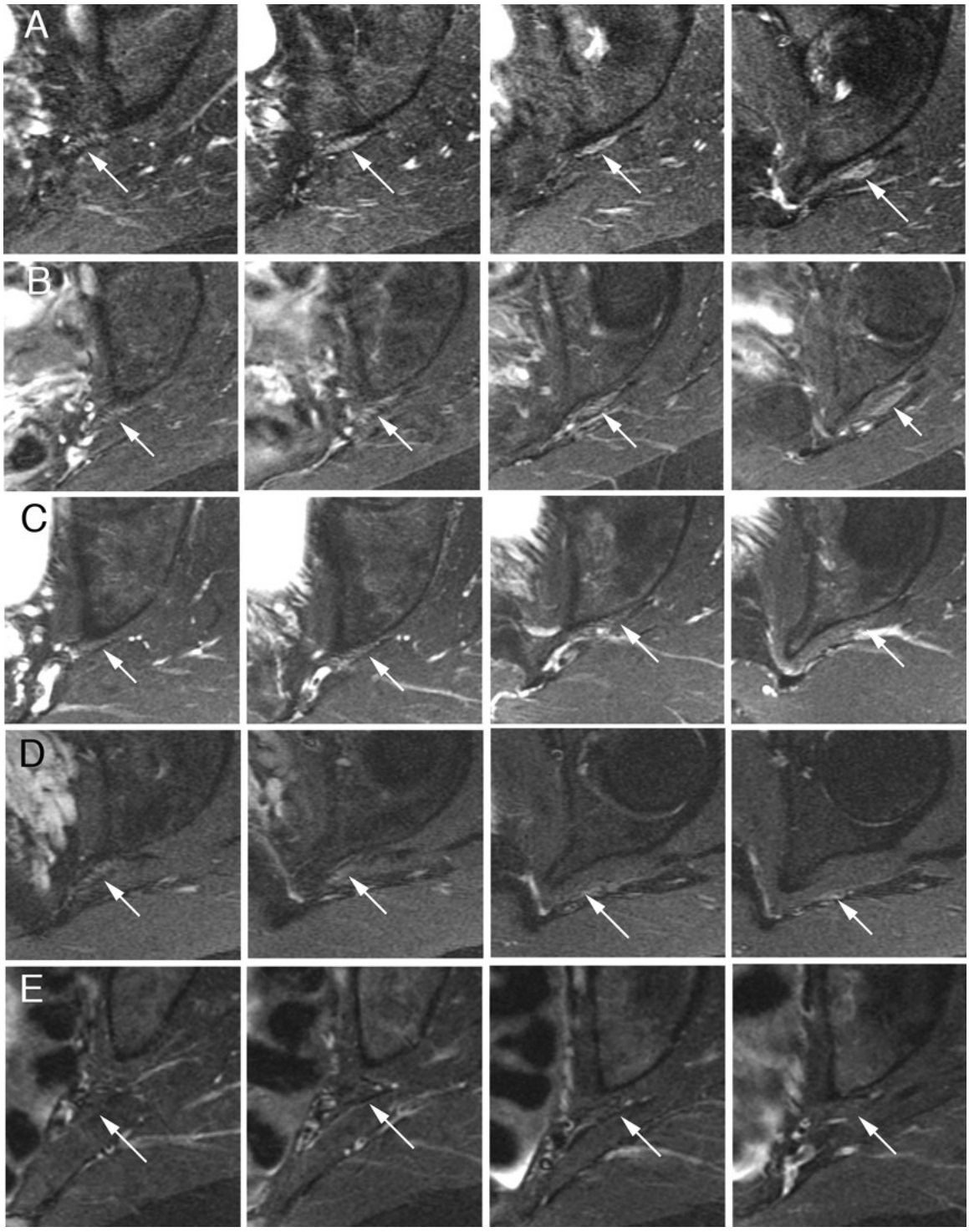

Figure 9 - Comparison of sciatic nerve appearance at the sciatic notch in patients with hyperintensity and in normal patients. Cases A and B demonstrate hyperintensity in the sciatic nerve in a series of images as the nerve exits the sciatic notch and

descends below the level of the piriformis tendon. In normal cases C, D, E the sciatic nerve is nearly isointense with surrounding muscle tissue. Sciatic nerve indicated by arrow in all images.

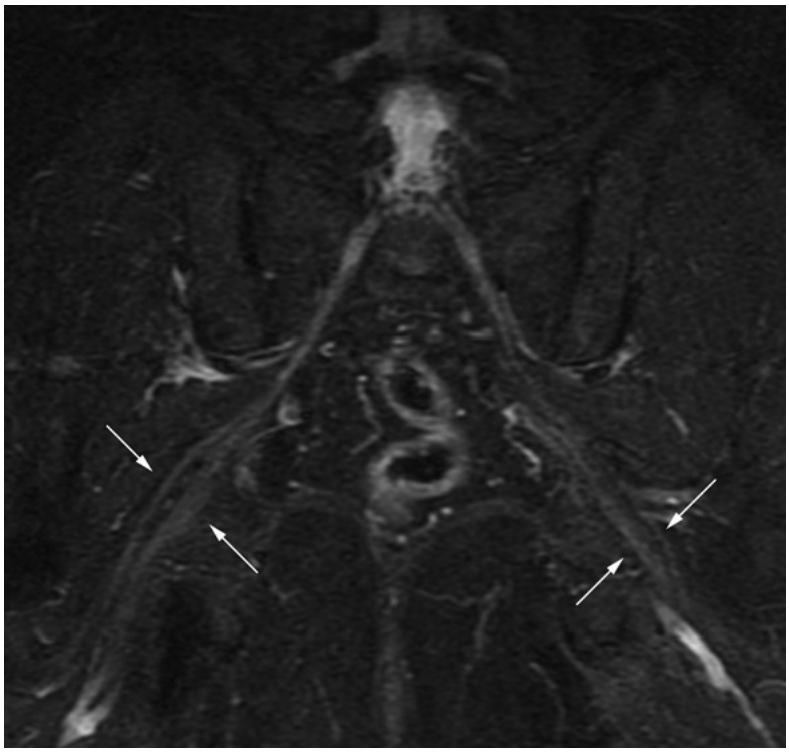

Figure 10 – Bilateral split sciatic nerve at piriformis muscle in patient with bilateral piriformis syndrome. Among the most important aspects of pre-operative planning in management of sciatic nerve entrapments in the pelvis is the identification of patients with a split sciatic nerve partly passing through the piriformis muscle. This image demonstrated the S1 spinal roots, spinal nerves, LS plexus, and split peroneal and tibial components of the sciatic nerve (arrows) as they are deviated by segments of the piriformis muscle bilaterally.

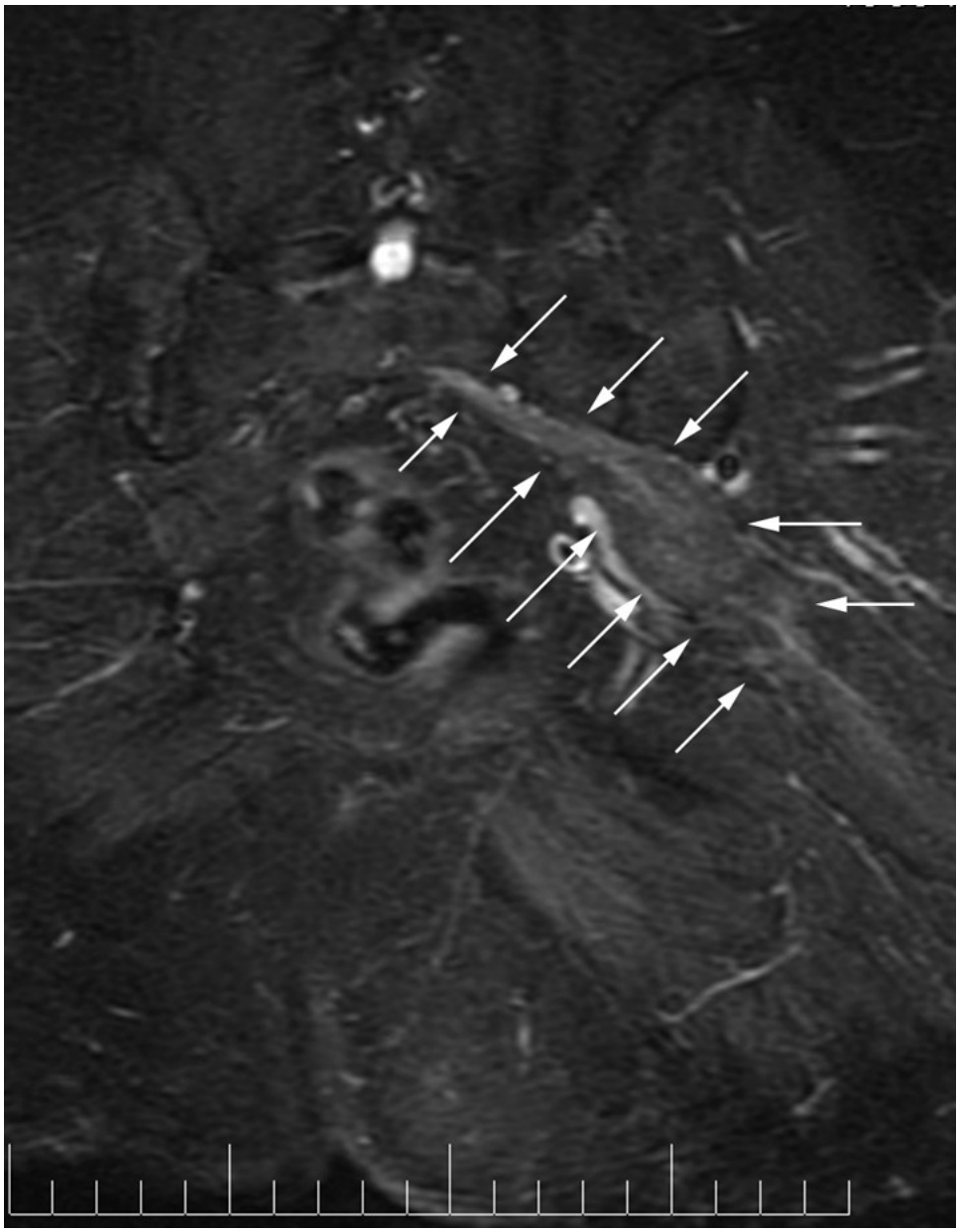

Figure 11 – Severe focal compression of the sciatic nerve at the sciatic notch. The nerve is flattened, hyperintense and expanded to more than twice its normal diameter. This is a post-operative result that occurred when only one of the two bipartite

elements of the piriformis muscle was released in a patient with split nerve and split muscle. Differential retraction of the cut piriformis segment relative to the intact segment caused a severe mechanical impingement syndrome.

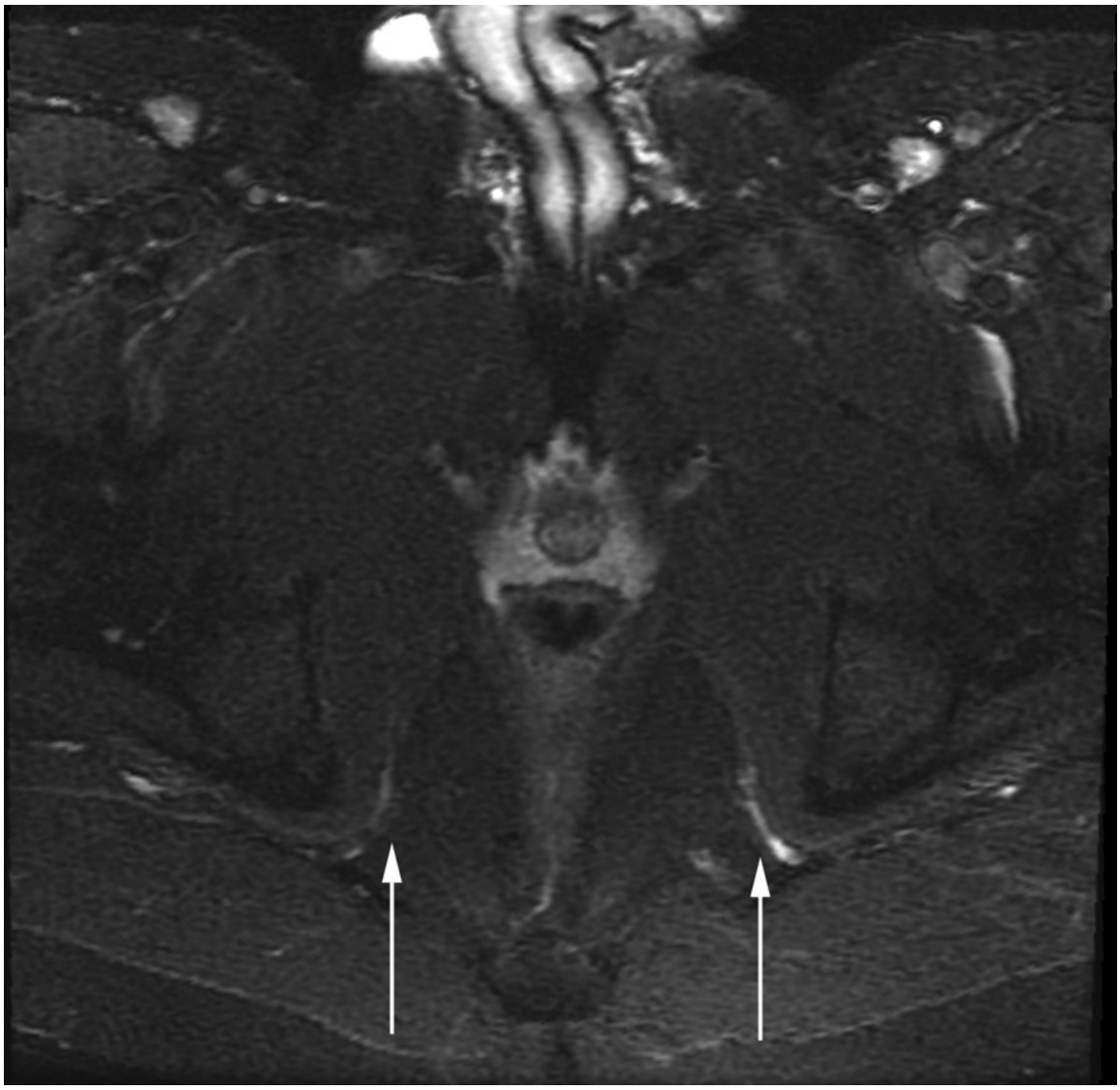

Figure 12 – Pudendal nerve entrapment between the ischial spine and the Alcock canal.

In patients with unilateral pudendal entrapment in the Alcock canal, it is typical to

see asymmetric swelling and hyperintensity affecting the pudendal neurovascular bundle. Note increased caliber and hyperintensity at the left pudendal nerve indicated by the left arrow. Figure reproduced with permission from: Filler AG: Diagnosis and management of pudendal nerve entrapment syndromes: impact of MR Neurography and open MR-guided injections. **Neurosurgery Quarterly** 18:1-6, 2008 .

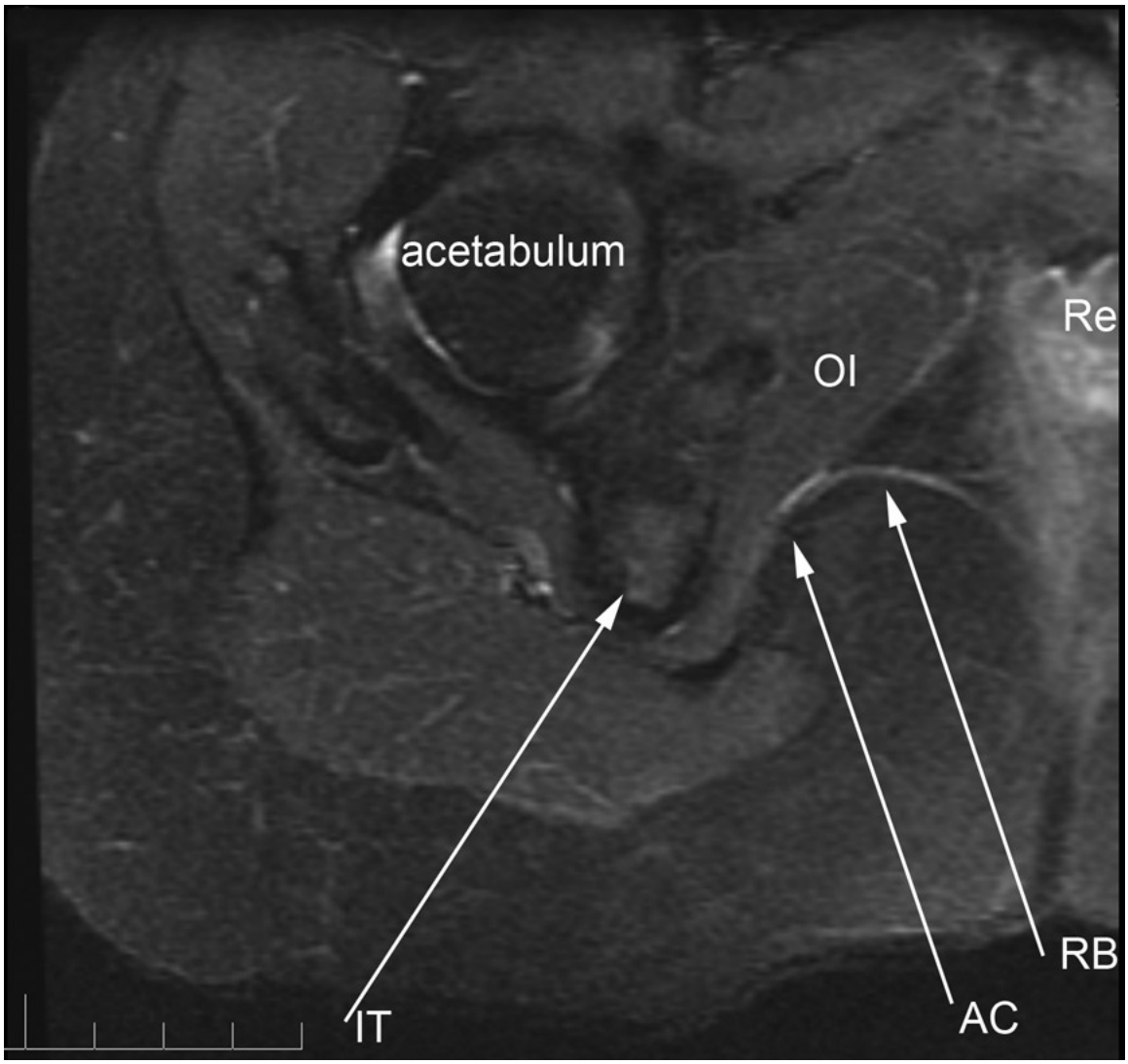

Figure 13 - Distal pudendal nerve neurographic image anatomy. The pudendal nerve in the Alcock canal (AC) runs along the medial aspect of the obturator internus muscle (OI) medial to the ischial tuberosity (IT). The rectal branch of the nerve (RB) is well seen in most imaging cases (Re = rectum). Figure reproduced with permission from: Filler AG: Diagnosis and management of pudendal nerve entrapment syndromes: impact of MR Neurography and open MR-guided injections. **Neurosurgery Quarterly** 18:1-6, 2008 .

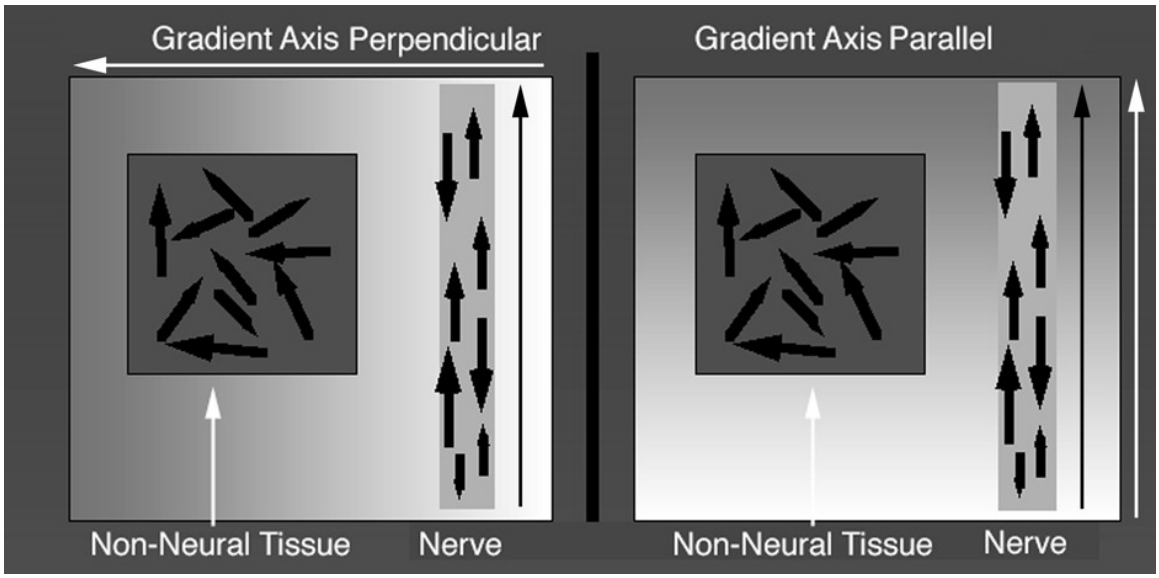

Figure 14 - Isotropic and anisotropic diffusion of water molecules in diffusion MRI. Shades of gray intensity indicate the intensity of the magnetic field which varies across the image plane due to the imposed pulsed magnetic field gradient. Water diffuses in all directions in most non-neural tissues (isotropically) but diffuses preferentially along the long axis of nerves (anisotropically). When all the water molecules in a tissue experience identical magnetic field strength despite diffusion movements, the MR signal from that tissue remains bright relative to the signal decay in surrounding isotropically diffusing tissue water. This is the situation on the left where the magnetic gradient is oriented perpendicular to the nerve. In the situation on the right, the water molecules in nerve move

preferentially to different positions in the gradients more rapidly than in the non-neural tissue so that the signal remains brighter from non-neural tissue.

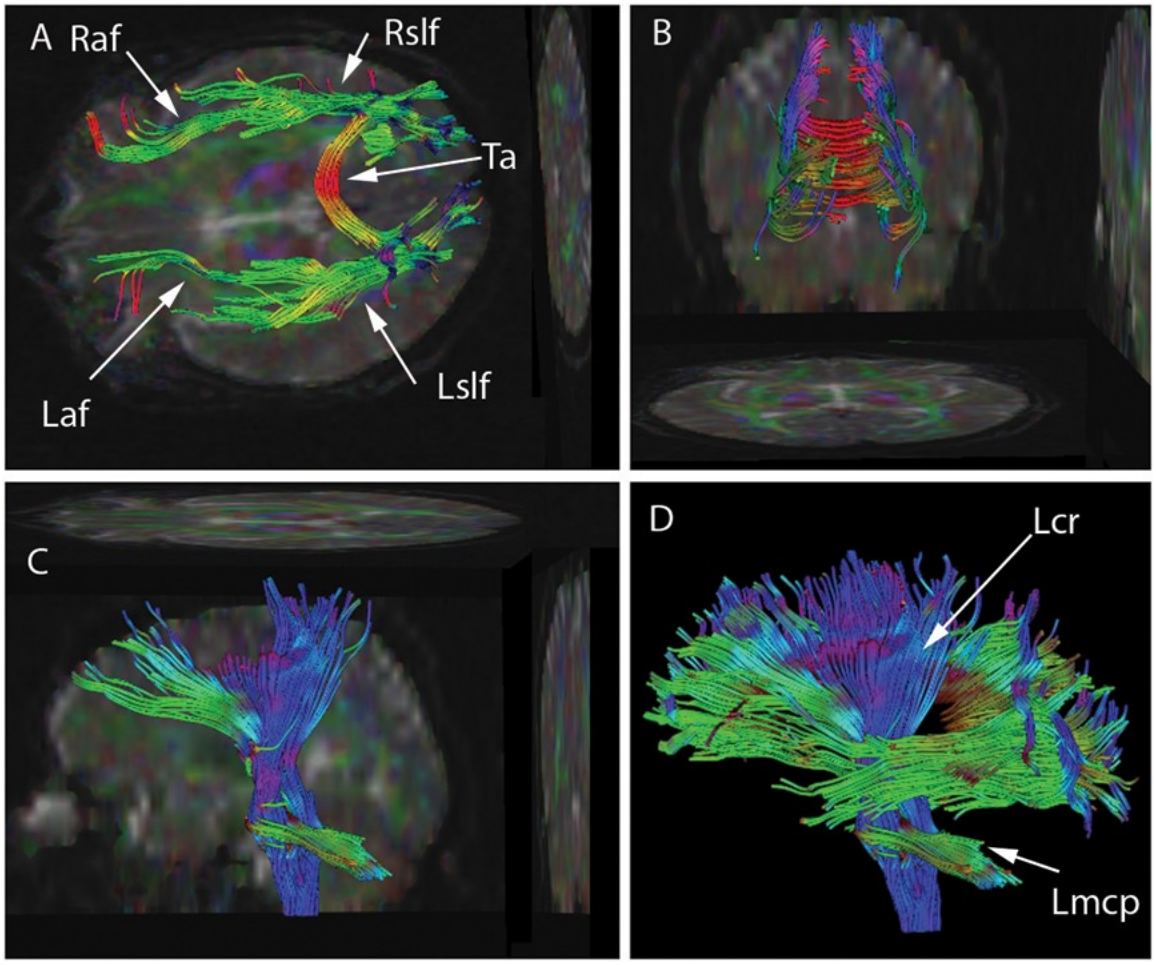

Figure 15 - Diffusion tensor imaging (DTI) data has been used to seed various tractographic assessments of this patient's brain. These are seen in superior (A), posterior (B), and lateral views (C&D). The seeds have been used to develop arcuate and superior longitudinal fasciculi in (A) and (B), for brainstem, and corona radiata in (C), and as combined data sets in (D). Some of the two

dimensional projections of the tractographic result are also shown. The data set may be rotated continuously into various planes to better appreciate the structure. Color has been assigned based on the dominant direction of the fibers. There is asymmetry in the tractographic fiber volume between the right and left arcuate fasciculus (Raf & Laf) (smaller on the left) and between the right and left superior longitudinal fasciculus (Rslf & Lslf) (smaller on the right). Also seen are Tapetum (Ta), Left corona radiata (Lcr) and Left middle cerebellar peduncle (Lmcp).

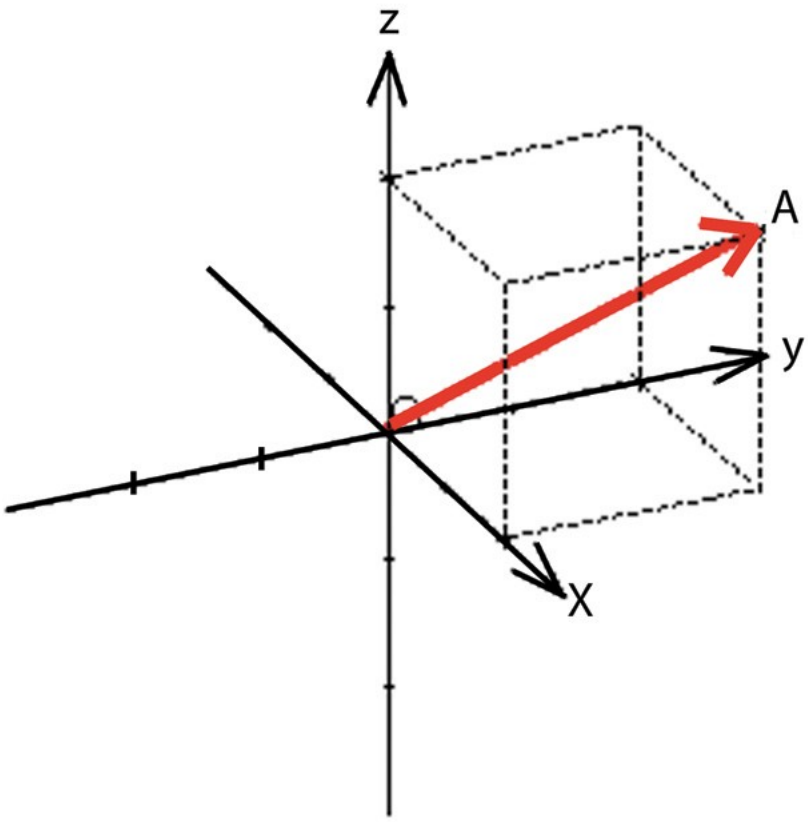

Figure 16 - A Cartesian orthogonal frame of reference depicting Vector A.

The measurement of the projection of this vector onto each of the three axes, X, Y and Z is two units. Because all of the measurements are positive, the vector (A) points into the octant of space bound on each side by the positive half of each axis.

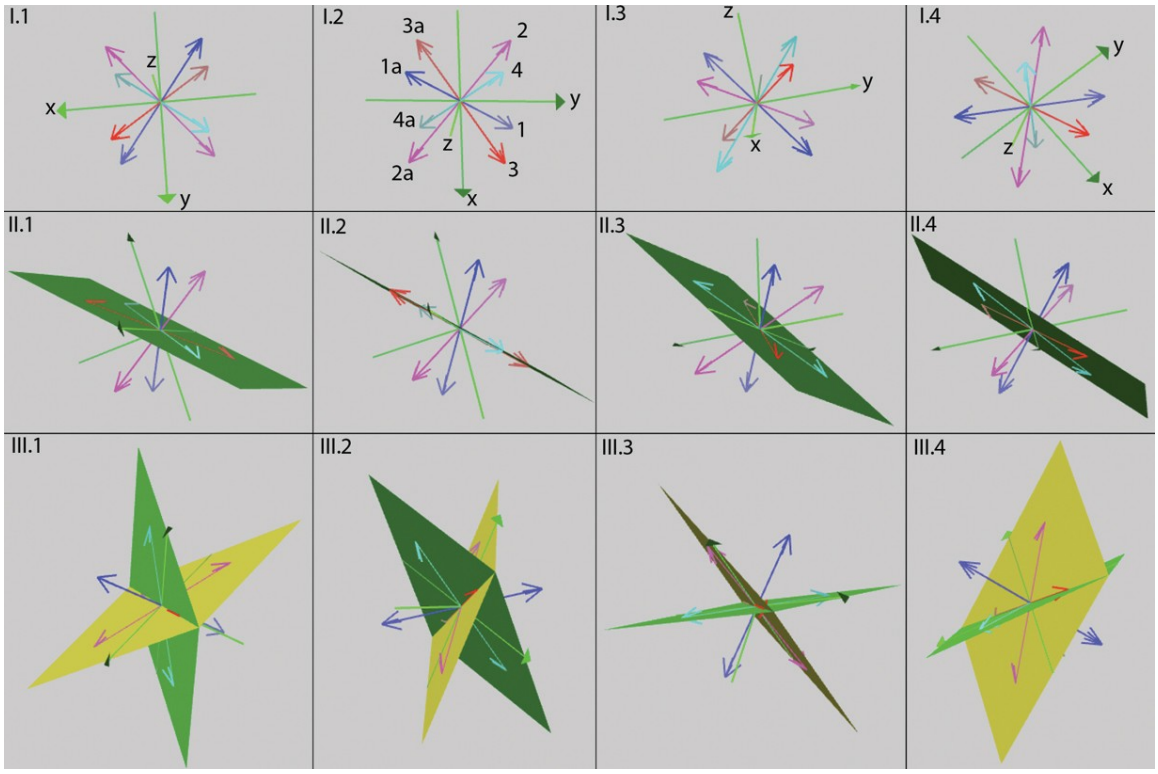

Figure 17 - Explanation of Anti-Symmetric Dyadic Tensor

For each of three graph series (I - III) there are four different rotations shown to help with visualization.

I) For diffusion measurements along each axis, the direction (sign) is not known. In this example the neural tract is running along the diagonal of the voxel so the measurements on X, Y and Z are equal. As shown, the ambiguity leads to eight possible vectors (1 & 1a - blue; 2 & 2a - purple; 3 & 3a - red; 4 & 4a turquoise) along the four diagonals of the space. This uncertainty arises when only three orthogonal diffusion directions are measured. Each vector runs along a diagonal in one of the eight possible octants of this Cartesian space. We know that six of

the vectors must be artifactual "ghosts" but we must use three more diffusion gradient acquisition directions to distinguish the ghosts from the dyad that actually represents the true neural tract orientation.

II) To clarify the situations, two more gradient axes have been measured, each of which was oriented along one of the diagonals of the space. A green plane determined by these two new measurement lines has been drawn. Notice that this plane incorporates the red (3 & 3a) and the turquoise (4 & 4a) vector pairs. Because our measurement was near zero in these two directions, we can discard the four vectors in these four octants.

III) A sixth gradient measure has now been made. This also had a very low intensity (rapid decay) we know we can discard the two vectors in these two octants as well. A yellow plane that incorporates the red (3 & 3a) and the purple (2 & 2a) vectors is shown to demonstrate how the actual vector can have length along all six Cartesian axes but not be zeroed by the two diagonal planes. Notice that by observing the various rotations, we see that the dyad made up of the blue vectors (1 and 1a) runs in the octants that remain. This shows how six measurements can orient the dyad and determine which of four possibilities is the true tractographic course.

Acknowledgements

The author would like to thank David Kline, H. Richard Winn, B. Anthony Bell, David Uttley, John Griffiths, Andrew Lever, Hermann Hauser, Franklyn Howe, Todd Richards, Jim Nelson, Ken Maravilla, Terrence Deacon, Jodean Peterson, and Shirlee Jackson, for their assistance, contributions and inspiration in the course of this effort. Franklyn Howe is also thanked for comments on math and physics discussions in the text of this article. Pioneering work and teaching in axonal tracer science by Walle J.H. Nauta at MIT and Richard L. Sidman at Harvard Medical School also provided inspiration for the early stages of conception of this endeavor. Portions of this work were supported by NIH PHS #5 T32 GM07117-09 0011 (Harvard), NIH NSTG 5T32 NS-07144-09 (University of Washington), UK Dept. Trade & Industry (DTI) Smart Award, The Wellcome Trust "MR Imaging of Neural Tracts", the UK Cancer Research Campaign, and the Neurosciences Research Foundation of Atkinson Morley's Hospital.

Financial Disclosure

Aaron G. Filler, MD, PhD is a co-inventor on patents that cover the use of MR Neurography and DTI imaging. He has received funding from NIH, The Wellcome Trust, and the Atkinson Morley's Research Foundation for scientific

research related to the subject matter. His clinical neurosurgical practice employs these imaging techniques. He performs radiology interpretations on MR Neurography and DTI images. He is a shareholder in NeuroGrafix – a company that administers patent technology licenses under agreement from the University of Washington which owns the patent and which also manages image data transport for neural tract imaging although he has not received any funds from NeuroGrafix.

Authorship

Aaron Filler, MD, PhD, FRCS was the primary investigator in this research, conceived of the research plan, invented the technologies, carried out the clinical implementation, participated directly in the imaging and image interpretation process. He generated the text and figures personally and also assembled the manuscript.

Article Summary

It is now possible to use MRI scanning to provide detailed images of nerves as well as neural tracts in the brain. This greatly extends the capabilities of imaging to assist in the diagnosis of nearly every category of neurological disorder. The impact of nerve and neural tract imaging is now becoming clear as summary evaluation of the kinds of information these tests provides becomes available. In the future, imaging of nerves and neural tracts of the brain will play an increasingly important role in the diagnostic process and they promise to offer specific results in areas where current diagnostic methods have often been insufficient.